

PAPER • OPEN ACCESS

The study of crystallization of Mg-based bulk metallic glass (BMG)

To cite this article: A. I. Ismail *et al* 2019 *IOP Conf. Ser.: Mater. Sci. Eng.* **494** 012080

View the [article online](#) for updates and enhancements.



IOP | ebooks™

Bringing you innovative digital publishing with leading voices to create your essential collection of books in STEM research.

Start exploring the [collection](#) - download the first chapter of every title for free.

The study of crystallization of Mg-based bulk metallic glass (BMG)

A. I. Ismail^{1,2}, R. Haliq¹, M. Jamil¹

¹ Mechanical Engineering, Institut Teknologi Kalimantan, Balikpapan, Indonesia

² National Center for Sustainable Transportation Technology (NCSTT), Bandung, Indonesia

E-mail: a.idhil@itk.ac.id

Abstract. Bulk metallic glass (BMG) is an excellent candidate for future material in various applications due to its superior physical and mechanical properties. The characterization of the crystallization evolution of Mg₅₈Cu₃₁Gd₁₁ has been performed using in-situ synchrotron radiation technique. Differential scanning calorimeter (DSC) and laboratory X-ray diffraction were also implemented to confirm the crystallization during heating at 20 °C/min. The glass transition temperature (T_g) was resolved and the occurrence of two stages crystallization was found during the process. The Mg₂Cu growth accompanies the crystallization process and occurrence of more complex compound is suggested.

Keyword: crystallization, Mg-based, bulk metallic glass, study

1. Introduction

Mg-based bulk metallic glass (BMG) alloys have given high attraction due to the precious properties of these alloys. The search for new magnesium-based alloys is of great economic interest due to their advantages such as light weight, great abundance and good corrosion resistance [1]. Most of the BMG alloys are based on the ternary or pseudo-ternary systems [2,3] in which additional or substituting elements are introduced. Therefore, it is important to study the ternary systems by locating the best glass-forming compositions before expanding the research into multicomponent systems. Mg-based ternary bulk metallic glasses with high glass forming ability (GFA) and wide supercooled region have been developed in various number of alloys, the most widely developed is Mg-TM-RE (TM = Transition metal, such as Ni, Cu, and Zn). Some series of Mg-Cu-RE BMGs system (RE = Rare earth elements, for example: La, Ce, Er, Gd, Te, Nd, Pr, Dy, Yb, and Sm) have been researched [4,5].

The first development of Mg-Based bulk metallic glass was performed by Inoue and co-workers, they reported the formation of Mg-based amorphous alloys in Mg-Cu-Y system with high glass forming ability [6]. The Mg₆₅Cu₂₅Y₁₀ composition (also called as Inoue alloy) was found to be the most favourable so that BMG rods with a diameter of 4 mm could be fabricated via copper mould casting. The critical cooling rate of the BMG was estimated in the order of 50 Ks⁻¹. The researchers have shown the development of the GFA by additions or substitutions of elements in the Mg-based BMGs.

Liu and Lu [7] have reviewed the recent works regarding the effects of minor alloying additions on glass formation in bulk metallic glasses. Experimental evidences indicate that alloying additions of small atoms with atomic radius smaller than 0.12 nm such as Si or large atoms with radius greater than



0.16 nm such as Y are most effective in enhancing glass forming ability. A small amount Si addition provide an improvement of GFA. Without Si, 4 mm thick $\text{Ni}_{40}\text{Cu}_6\text{Ti}_{16}\text{Zr}_{28}\text{Al}_{10}$ strip shows an observable Bragg peak superimposed on the broad, amorphous diffraction band, indicating that small nanocrystals have precipitated from the amorphous matrix. However, with 0.5% Si, the alloy $(\text{Ni}_{40}\text{Cu}_6\text{Ti}_{16}\text{Zr}_{28}\text{Al}_{10})_{99.5}\text{Si}_{0.5}$ is fully amorphous up to 5 mm, as shown by the absence of any sharp crystalline.

Further development of GFA has been found in Mg-Cu-Y alloy system where Cu is substituted partially by elements such as Zn and Ag. Some examples of these alloys are $\text{Mg}_{65}\text{Cu}_{15}\text{Ag}_5\text{Pd}_5\text{Y}_{10}$ [8], $\text{Mg}_{65}\text{Cu}_{20}\text{Zn}_5\text{Y}_{10}$ [9,10], and $\text{Mg}_{65}\text{Cu}_{15}\text{Ag}_{10}\text{Y}_{10}$ [11]. Y and Gd have similar atomic radius (Y: 0.18015 nm Gd: 0.18013 nm), similar electronegativity and similar negative heat of mixing. The effect of substitution of Y with Gd in the $\text{Mg}_{65}\text{Cu}_{25}\text{Y}_{10}$ alloy produces significant improvement of the GFA, enabling the fabrication of the BMG with a diameter up to 8 mm by Cu mold casting method, possibly because of the difference in the electronic configurations between Y (4d 15s2) and Gd (4f 75d 16s2). In this study, it is intended to investigate the crystallization behaviour of Mg-Cu-Gd system in the case of $\text{Mg}_{58}\text{Cu}_{31}\text{Gd}_{11}$.

2. Experimental methods

2.1. Material preparation

The $\text{Mg}_{58}\text{Cu}_{31}\text{Gd}_{11}$ alloy is studied in this research. Mg is a very volatile element, therefore to ensure that the alloy form correct composition, an excessive amount of Mg about 6 wt% of the nominal composition was used in the starting mixture to avoid the decreasing of the Mg amount. Before starting the arc melting process, in order to avoid oxidation of the pure elements, the argon gas must be continuously purged into the arc furnace to flush the oxygen and then to achieve a low oxygen atmosphere environment inside the furnace. The process should be repeated several times to ensure high vacuum inside the furnace to protect from oxidization. In order to increase the heat exchange rate, cold water needs to be poured into and flowing through the bottom of the copper mold. Finally, the elements of alloy placed on the bottom of the copper mold will be melted by a high voltage arc under a Ti-gettered argon atmosphere in a water-cooled copper mould. It should be repeated several times for alloy ingots to confirm composition homogeneity. A melt spinning method was used to produce the amorphous alloy in ribbon form. Master alloy was put into the quartz tube. In chill block melt spinning, a molten liquid alloy was ejected by gas pressure onto a rapidly rotating wheel. Solidification occurs on the melt spinning wheel and results in the formation of ribbons, which detach easily from the wheel surface due to thermal contraction differences.

2.2. Measurement techniques

The bulk metallic glass is produced by copper mold casting method. The structure was investigated by using x-ray diffraction (XRD) either by using high energy synchrotron diffraction, conventional diffractometer, and scanning electron microscopy (SEM) including energy dispersive spectrometry (EDS). The thermal stability of the material was examined by using a differential scanning calorimeter (DSC). The structure of amorphous ribbons was confirmed by using conventional X-Ray diffraction (XRD) using Cu K α radiation; the crystallization behaviour of the amorphous alloy $\text{Mg}_{58}\text{Cu}_{31}\text{Gd}_{11}$ was examined using differential scanning calorimetry (DSC) with heating rate of 20 °C/min. Specimens for in-situ heating experiments, which were performed using synchrotron reach thickness for about 1 mm. The thick samples were then sealed under vacuum environment in quartz crucibles which contain Zr getter plates to increase the vacuum conditions. The energy of the photons applied was about ~90 KeV corresponding to a wavelength of 0.10947355 nm. The temperature of the sample was monitored with an infrared pyrometer up to ~297 °C.

3. Result and discussion

Figure 1 shows the XRD diffraction spectra of amorphous $\text{Mg}_{58}\text{Cu}_{31}\text{Gd}_{11}$ ribbon collected in transmission mode during induction heating, up to the temperature of ~297 °C in the monochromatic synchrotron beam. As we observe in the diffraction pattern, the glassy structure of the $\text{Mg}_{58}\text{Cu}_{31}\text{Gd}_{11}$

alloy was identified, consisting of a broad diffraction peak characteristic of the amorphous structure without any crystalline phase. The difference between the amorphousness and crystallization is obviously observed. X-axis represents the wave vector Q , given by $Q = (4\pi/\lambda) \sin \theta$. From the diffraction patterns evolution, the general overview of the transformation phase occurred during induction heating up to $\sim 297^\circ\text{C}$ can be observed. Below the first crystallization temperature (about 220°C) we can observe a broad halo at low diffraction vector which comes from the quartz sample

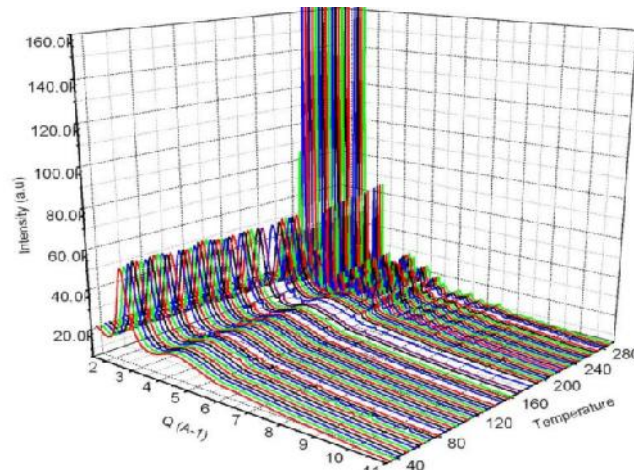


Figure 1. Diffraction pattern of amorphous phase a) and Differential Scanning Calorimetry (DSC) DSC curve for $\text{Mg}_{58}\text{Cu}_{31}\text{Gd}_{11}$ alloy during heating at the rate of $20^\circ\text{C}/\text{min}$.

holder, others halos are related to the amorphous phase. The pure amorphous phase could be clearly observed at the temperature from 30°C to 160°C as shown in Figure 2a.

From the diffraction patterns also can be seen that a primary phase starts to precipitate and produce many intense and narrow reflections with increasing temperature. It should be noted that there are still insufficient reports that clearly reviewed the crystallization behaviour of Mg-Cu-Gd system. Soubeyroux et al [12] produced $\text{Mg}_{65}\text{Cu}_{25}\text{Gd}_{10}$ and identified the formation of Mg_2Cu phase with the crystal size of about 100 nm. Small peaks with low intensities also appear in these spectra. In order to identify the intermetallic phases in $\text{Mg}_{58}\text{Cu}_{31}\text{Gd}_{11}$, the samples were heated in DSC up to melting temperature and an XRD pattern was recorded in a conventional diffractometer and more reflections of low intensity could be observed.

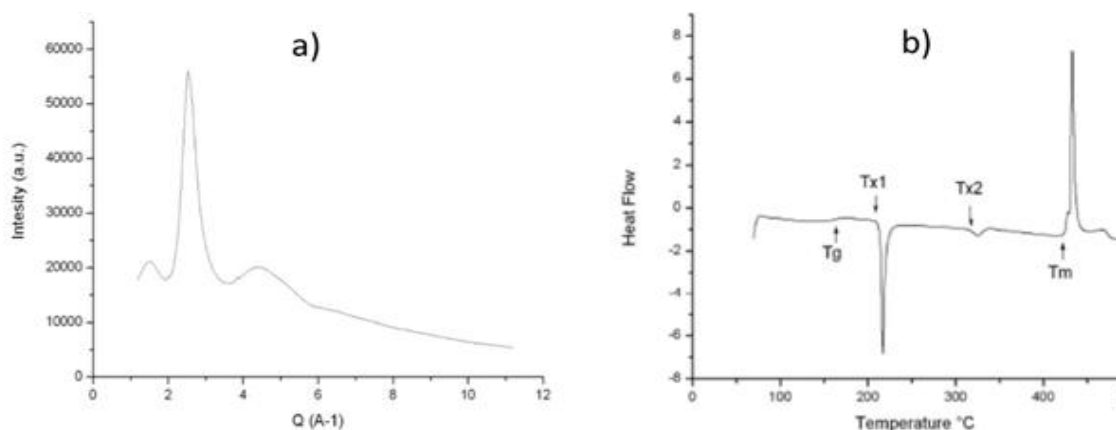


Figure 2. Diffraction pattern of amorphous phase a) and Differential Scanning Calorimetry (DSC) DSC curve for $\text{Mg}_{58}\text{Cu}_{31}\text{Gd}_{11}$ alloy during heating at the rate of $20^\circ\text{C}/\text{min}$.

Figure 2b shows the DSC results of the $Mg_{58}Cu_{31}Gd_{11}$ amorphous alloy heated up to melting temperature with the heating rate of $20\text{ }^{\circ}\text{C}/\text{min}$. From DSC measurement showed on Figure 2b, it is clearly justified an endothermic peak event associated to the glass transition at the temperature about $174\text{ }^{\circ}\text{C}$ and a sharp exothermic peak indicating crystallization process at the temperature around $220\text{ }^{\circ}\text{C}$. However, on the DSC result we can find also a second small exothermic peak in temperature around $320\text{ }^{\circ}\text{C}$. This peak confirms that crystallization process occurs through two stages process T_{x1} and T_{x2} . The second crystallization is mainly caused by some residual amorphous phase. Two steps of crystallization process are also confirmed by experimental pattern from in-situ measurement.

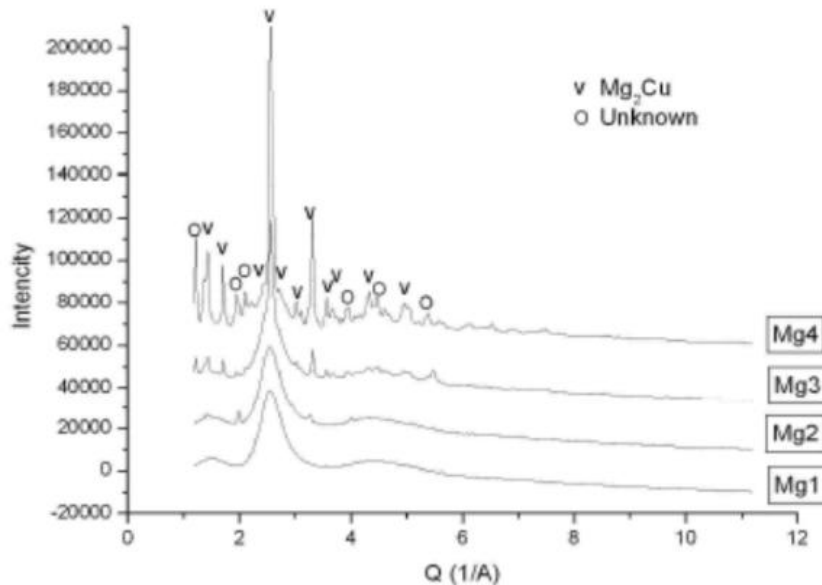


Figure 3. Sequence of diffraction patterns showing the transformation from amorphous phase to partially crystalline, and fully crystalline state.

Figure 3 demonstrates the clear evolution of phase transformation during in-situ experiment. Mg1 pattern justifies the amorphous state of the alloy. Some small peaks appear in the Mg2 pattern, which indicates that crystallization is occurring in some part of the alloy. These peaks are identified as Mg_2Cu compound according to calculated pattern. The peaks in Mg2 are still existing in Mg3 where the heating temperature reach about $178\text{ }^{\circ}\text{C}$ followed by the growing of peaks with higher intensity associated to an amorphous phase. When the temperature increases until $297.7\text{ }^{\circ}\text{C}$, the alloy becomes fully crystalline confirmed with the absence of amorphous halo as we find in pattern that is marked with Mg4. However, the halfwidth of the pattern also increases which directly corresponds to the broadening of the peak. It should be noted that the peak broadening can depend on the chemical homogeneity of the alloy because the lattice parameter variations are due to the chemical inhomogeneity. Moreover, the crystal/amorphous phase interfaces have a high level of stresses induced by volume effect of crystallization. In some cases, these stresses lead to the formation of twin peak in the growing crystals.

Figure 4 displays the comparison between annealed master alloy, unannealed master alloy pattern and crystallized pattern obtained by synchrotron diffraction. The diffraction pattern shows a match result of main peak between the patterns obtained from conventional x-ray and synchrotron diffraction. This informs us that the size and shape of the unit cell of the phases are generally the same. More peaks are also observed in the pattern and most of them are identified as Mg_2Cu phase. On the other hand, the diffraction pattern from undergoes broadening. Some very high peaks compared to the two patterns are also observed. In the annealed pattern, for position about 2.8 (marked with bigger star), as peak is growing to a very high intensity which could be a preferred orientation as the effect of

annealing for long term. This peak position is also corresponding to the position of 2.288 Å and 080 hkl index.

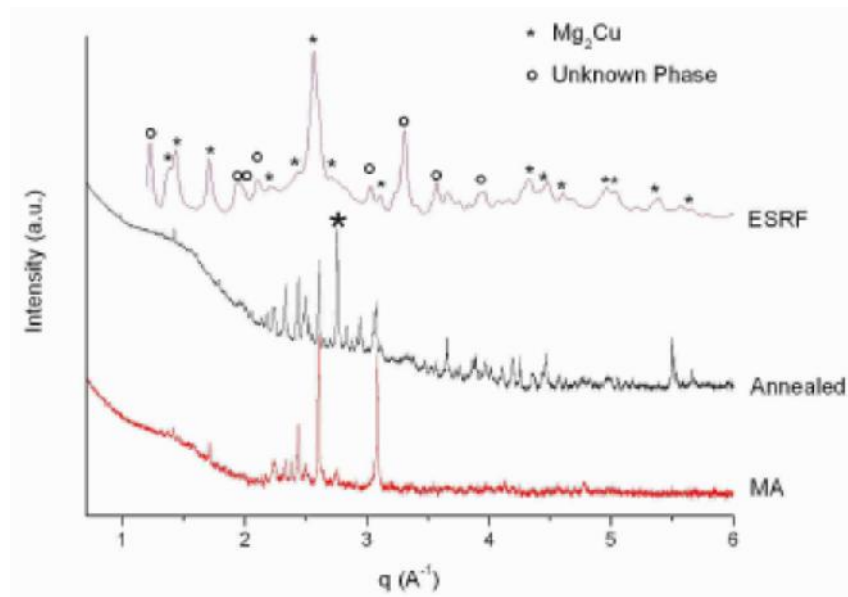


Figure 4. Diffraction pattern of three different BMG specimens obtained using laboratory XRD and Synchrotron.

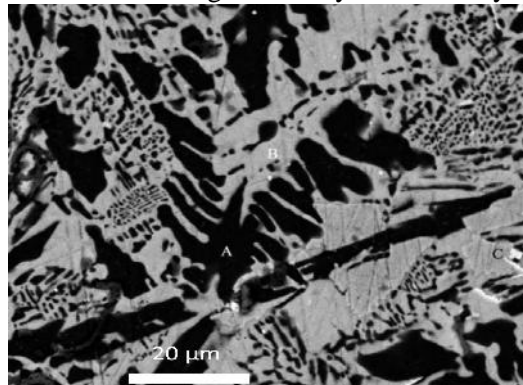


Figure 5. Microstructure of BMG after crystallization.

To confirm this phenomena SEM observations have been done in the annealed master alloy as shown in Figure 5. The SEM and EDS results show three phases formed during crystallization process. First phase, marked with A (black image) is identified as binary Mg_2Cu phase whose average crystal size is around 10 μm . Some larger crystals are also found in the alloy. Second phase is marked with B, with grey colour is identified as unknown phase, the third phase with white colour and brighter is also identified as unknown phase. This third phase contains large amount of Gd element which was probably not completely melted during the production of alloy due to characteristic of Gd that is difficult to melt.

4. Conclusion

In summary, we have conducted the investigation on the crystallization process of $Mg_{58}Cu_{31}Gd_{11}$ bulk metallic glass (BMG) by using various techniques. We found that the high energy x-ray diffraction patterns show crystallization process of $Mg_{58}Cu_{31}Gd_{11}$ alloy. Primary phase which is identified as

Mg₂Cu starts to grow at temperature ~178 °C and it is stable until the end of crystallization process. After annealing at isothermal temperature ~384 °C, some new peaks are found at higher two theta position. Most peaks are related to Mg₂Cu. This is confirmed with the XRD experiment after annealing sample. DSC measurement reveal two steps of crystallization. However, the second crystallization is due to residual of amorphous structure. T_g is ~174 °C and T_{x1} is ~220 °C. Using SEM and EDS measurement of master alloy, it can be concluded that there are three phases that were growing and stable inside the Mg₅₈Cu₃₁Gd₁₁ alloy. The first is Mg₂Cu, the other is unknown ternary phase, which requires more complex analysis to solve.

Acknowledgments

The authors thank to MAMASELF for the scholarship. The authors also acknowledge the National Center for Sustainable Transportation Technology (NCSTT) Bandung, Indonesia for the research support.

References

- [1] Yuan, G. and Inoue, A. 2005. The effect of Ni substitution on the glass-forming ability and mechanical properties of Mg–Cu–Gd metallic glass alloys. *Journal of Alloys and Compound*. **387** pp 134-138.
- [2] Johnson. W.L. 1996. Fundamental aspects of bulk metallic glass formation in multicomponent alloys. *Material Science Forum* **225-227** pp 35-50
- [3] Miracle, D.B. 2004. A structural model for metallic glasses. *Nature Materials* **3** pp 697-702
- [4] Xi, X.K., Zhao, D.Q., Pan, M.X. and Wang, W.H. 2005. On the criteria of bulk metallic glass formation in MgCu-based alloys. *Intermetallics* **13** pp 638-641.
- [5] Xi, X.K., Wang, R.J., Zhao, D.Q., Pan, M.X. and Wang, W.H. 2004. Glass forming Mg-Cu-RE alloys with strong oxygen resistance in manufacturability. *Journal of Non-Crystalline Solids*, **344** pp 105-109.
- [6] Inoue, A., Kato, A., Zhang, T., Kim, S.G. and Masumoto T. 1991. Mg-Cu-Y amorphous alloys with high mechanical strength produced by a metallic mold casting method. *Materials Transactions JIM* **32** pp 609-616.
- [7] Liu, C.T. and Lu, Z.P. 2005. Effect of minor alloying additions on glass formation in bulk metallic glasses. *Intermetallics* **13** pp 415-418.
- [8] Amiya, K. and Inoue, A. 2000. Thermal stability and mechanical properties of Mg-Y-Cu-M bulk amorphous alloys. *Materials Transactions JIM* **41** pp 1460-1462.
- [9] Men, H., Hu, Z.Q. and Xu, J. 2002. Bulk metallic glass formation in the Mg-Cu-Zn-Y system. *Scripta Materialia* **46** pp 699-703.
- [10] Yuan, G., Zhang, T. and Inoue, A. Synthesis and magnetic properties of Fe-Ni alloys particles obtain by hydrothermal reaction. 2004. *Material Letter* **58** pp 3012-3016.
- [11] Park, E.S., Kang, H.G., Kim, W.T. and Kim, D.H. 2001. The effect of Ag addition in the glass forming ability of Mg-Cu-Y metallic glass alloys. *Journal of Non-Crystalline Solids* **279** pp 154-160.
- [12] Soubeyroux, J.-L., Puech, S. and Blandin, J.-J. 2007. Preparation of soft magnetic Fe-Ni_{pb}-B alloy nanoparticles by room temperature. *Material Science and Engineering A* **449-451** pp 248-253